

D303

MOLECULAR DYNAMICS SIMULATION OF HETEROGENEOUS NUCLEATION OF LIQUID DROPLET ON SOLID SURFACE

Tatsuto Kimura* and Shigeo Maruyama**

*Department of Mechanical Engineering, The University of Tokyo
7-3-1 Hongo, Bunkyo-ku, Tokyo 113-8656, Japan

**Engineering Research Institute, The University of Tokyo
2-11-16 Yayoi, Bunkyo-ku, Tokyo 113-8656, Japan

ABSTRACT The heterogeneous nucleation of liquid droplet on a solid surface was simulated with the molecular dynamics method. Argon vapor was represented by 5760 Lennard-Jones molecules and the solid surface was represented by one layer of 1020 harmonic molecules with the constant temperature heat bath model using the phantom molecules. The potential parameter between solid molecule and vapor molecule was changed to reproduce various surface wettabilities. After the equilibrium condition at 160 K was obtained, temperature of the solid surface was suddenly set to 100 K or 80 K by the phantom molecule method. The observed nucleation rate, critical nucleus size and free energy needed for cluster formation were not much different from the prediction of the classical heterogeneous nucleation theory in case of smaller cooling rate. The difference became considerable with the increase in cooling rate and with increase in surface wettability because of the spatial temperature distribution.

Keywords: Molecular Dynamics Method, Heterogeneous Nucleation, Liquid Droplet, Lennard-Jones Potential

1. NOMENCLATURE

$c(n)$: Number distribution function of clusters
 f : Function in classical heterogeneous nucleation theory
 J : Nucleation rate, $\text{cm}^{-2}\text{s}^{-1}$
 k : Spring constant, N/m
 k_B : Boltzmann constant, J/K
 m : Mass, kg
 n : Cluster size
 R_0 : Distance between nearest neighbor molecules, m
 r : Radius or distance between two molecules, m
 r_c : Cutoff radius, m
 S : Supersaturation ratio
 T : Temperature, K
 T_{wall} : Set temperature of phantom molecules, K

Greek Symbols

α : Damping factor, kg/s
 ΔG : Free energy needed for cluster formation, J
 Δt : Time step, s
 ε : Energy parameter of Lennard-Jones potential, J
 $\varepsilon_{\text{SURF}}$: Depth of integrated effective surface potential, J
 ϕ : Potential function, J
 ϕ_{SF} : Shifted Lennard-Jones potential function, J
 γ_{lv} : Surface tension of liquid vapor interface, N/m
 θ : Contact angle, rad
 ρ : Number density, m^{-3}
 σ : Length parameter of Lennard-Jones potential, m
 σ_F : Standard deviation of exciting force, N

Subscripts and superscripts

AR: Argon
ave: Average over nucleation period
e: Saturated vapor
INT: Interaction between argon and solid molecules
l: Liquid
S: Solid molecule
sim: Simulation
th: Classical nucleation theory
*: Critical nucleus

2. INTRODUCTION

The liquid droplet nucleation on a solid surface is very important phenomena from the viewpoint of the dropwise condensation theory, and is also very interesting phenomena related to the nanotechnology such as the quantum dot generation. We simulated the equilibrium liquid droplet on the solid surface by the molecular dynamics method, and have clarified the relationship between potential parameter of molecules and macroscopic quantities such as contact angle [1]. In addition, we have carried out the molecular dynamics simulation on the bubble nucleation process on the solid surface [2]. In the meantime, direct molecular dynamics simulations of the homogeneous nucleation process were performed by Yasuoka et al. for the Lennard-Jones fluid [3] and water [4], and a large discrepancy from the classical nucleation theory was reported. Here, the heterogeneous nucleation of liquid droplet on solid surface was directly simulated by the molecular dynamics method and the nucleation rate was compared with the classical nucleation theory.

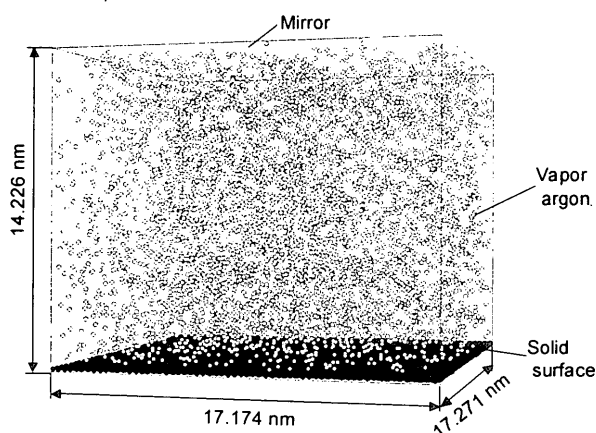


Figure 1 Simulation system.

3. SIMULATION METHOD

As shown in Figure 1, vapor argon consisted of 5760 molecules in contact with plane solid surface was prepared. The potential between argon molecules was represented by the well-known Lennard Jones (12-6) function as

$$\phi(r) = 4\epsilon \left\{ \left(\frac{\sigma}{r} \right)^{12} - \left(\frac{\sigma}{r} \right)^6 \right\} \quad (1)$$

where the length scale $\sigma_{AR} = 3.40 \times 10^{-10}$ m, energy scale $\epsilon_{AR} = 1.67 \times 10^{-21}$ J, and mass $m_{AR} = 6.63 \times 10^{-26}$ kg. We used the potential cut-off at $3.5\sigma_{AR}$ with the shift of the function for the continuous decay [5].

$$\begin{aligned} \phi_{SF}(r) = 4\epsilon \left\{ \left[\left(\frac{\sigma}{r} \right)^{12} - \left(\frac{\sigma}{r} \right)^6 \right] \right. \\ \left. + \left[6 \left(\frac{\sigma}{r_c} \right)^{12} - 3 \left(\frac{\sigma}{r_c} \right)^6 \right] \left(\frac{r}{r_c} \right)^2 \right. \\ \left. - \left[7 \left(\frac{\sigma}{r_c} \right)^{12} - 4 \left(\frac{\sigma}{r_c} \right)^6 \right] \right\} \quad (2) \end{aligned}$$

The solid surface was represented by one layer of 1020 harmonic molecules in fcc (111) surface. Here, we set as: mass $m_S = 3.24 \times 10^{-27}$ kg, distance of nearest neighbor

molecules $R_0 = 2.77 \times 10^{-10}$ m, and the spring constant $k = 46.8$ N/m from the physical properties of solid platinum crystal. We have controlled the temperature of the solid surface by arranging a layer of phantom molecules beneath the 'real' surface molecules. The phantom molecules modeled the infinitely wide bulk solid kept at a constant temperature T_{wall} with proper heat conduction characteristics [6, 7]. In practice, a solid molecule was connected with a phantom molecule with a spring of $2k$ in vertical direction and springs of $0.5k$ in two horizontal directions. Then, a phantom molecule was connected to the fixed frame with a spring of $2k$ and a damper of $\alpha = 5.184 \times 10^{-12}$ kg/s in vertical direction and springs of $3.5k$ and dampers of α in two horizontal directions. A phantom molecule was further excited by the random force in gaussian distribution with the standard deviation

$$\sigma_F = \sqrt{\frac{2\alpha k_B T}{\Delta t}} \quad (3)$$

where k_B is Boltzmann constant. This technique mimicked the constant temperature heat bath, which conducted heat from and to 'real' surface molecules as if a bulk solid was connected.

The potential between argon and solid molecule was also represented by the Lennard-Jones potential function. The length scale of the interaction potential σ_{INT} was kept constant as 3.085×10^{-10} m. This value that should be another parameter of solid-fluid interaction, was temporarily fixed as $(\sigma_{AR} + R_0)/2$ as Ref. [1]. In our previous study on the liquid droplet on the surface [1], we have found that the depth of the integrated effective surface potential

$$\epsilon_{SURF} = \frac{4\sqrt{3}\pi}{5} \frac{\epsilon_{INT} \sigma_{INT}^2}{R_0^2} \quad (4)$$

was directly related to the contact angle of the surface. Hence, we used various energy scale parameters ϵ_{INT} as shown in Table 1 to change the wettability.

The classical momentum equation was integrated by the Verlet's leap-frog method with the time step of 5 fs. As an initial condition, an argon fcc crystal was placed at the center of the calculation domain. We used the velocity-scaling temperature-control directly to argon molecules for initial 100 ps. Then, switching off the direct temperature control, the system was run for 500 ps with the temperature control only from the phantom molecules until

Table 1 Calculation conditions.

Label	ϵ_{INT} [$\times 10^{-21}$ J]	θ [deg]	T_{wall} [K]	T_{ave} [K]	J_{sim} [cm^2s^{-1}]	J_{th} [cm^2s^{-1}]
E1	0.426	135.4	100	108	6.52×10^{20}	4.86×10^{21}
E2	0.612	105.8	100	114	3.45×10^{21}	4.47×10^{21}
E3	0.798	87.0	100	120	5.76×10^{21}	5.54×10^{20}
E1-L	0.426	135.4	80	111	3.96×10^{21}	2.23×10^{21}
E2-L	0.612	105.8	80	126	1.41×10^{22}	(10^{-134})
E3-L	0.798	87.0	80	129	2.96×10^{22}	N-A

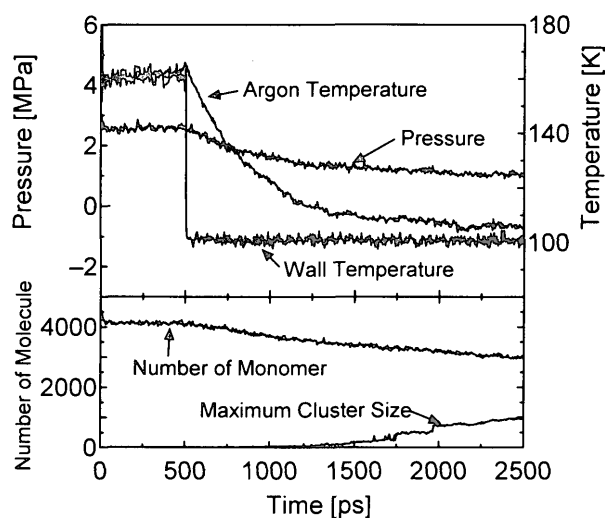


Figure 2 Variations of pressure, temperature, number of monomer and maximum cluster size for the case of E2.

the equilibrium argon vapor was achieved. After the equilibrium condition at 160 K was obtained, the set temperature of phantom T_{wall} was suddenly lowered to 100K or 80 K, and the system was cooled from the solid surface. The supersaturation ratio

$$S = \frac{\rho}{\rho_c} \quad (5)$$

was evaluated to be about 6 and 40 at this stage, respectively.

4. RESULTS AND DISCUSSIONS

Variations of argon temperature and pressure in response to the wall temperature change for E2 in Table 1 are shown in top panel of Figure 2. Here, we define the “cluster” as a interconnecting group of molecules whose intermolecular distances are less than $1.2\sigma_{AR}$. Change in number of monomer and maximum cluster size are plotted in Figure 2. In order to clarify the sensitivity to the threshold value of cluster definition, the following analyses were performed for another threshold value $1.5\sigma_{AR}$. As a result, no substantial differences were observed. After 500 ps from the start of the calculation, solid surface was rapidly cooled by the temperature control of phantom molecules, and the temperature of argon gradually decreased afterward, then the formation and growth of clusters were recorded.

In Figure 3, the snapshots of nucleation process for E2 are shown. Here, for clarity, only the clusters made of more than 5 molecules are shown. Initial small clusters appeared and disappeared randomly in space. Then larger clusters grew preferentially near the surface. Some of largest clusters near the surface continued to grow until the end of the simulation. On the other hand, for the less wettable condition E1 in Figure 4, relatively large clusters grew without the help of surface, similar to homogeneous

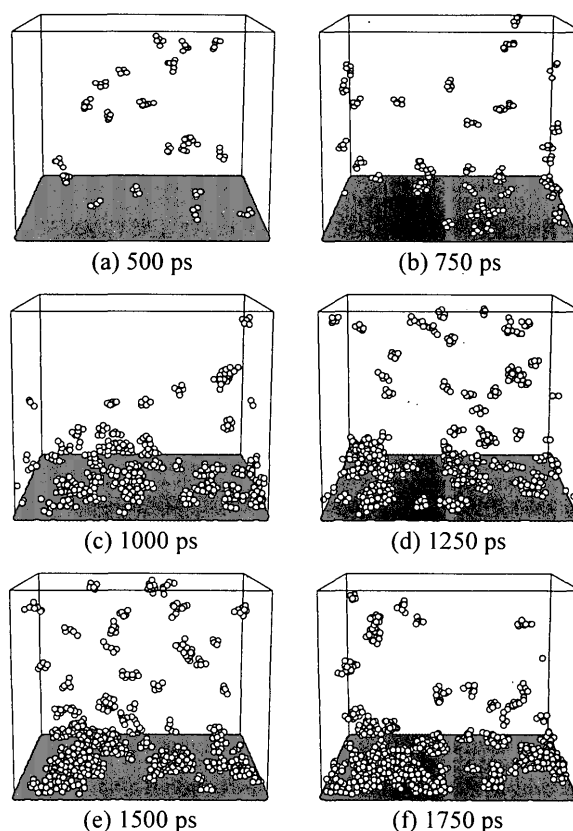


Figure 3 Snapshots of nucleation process for E2.

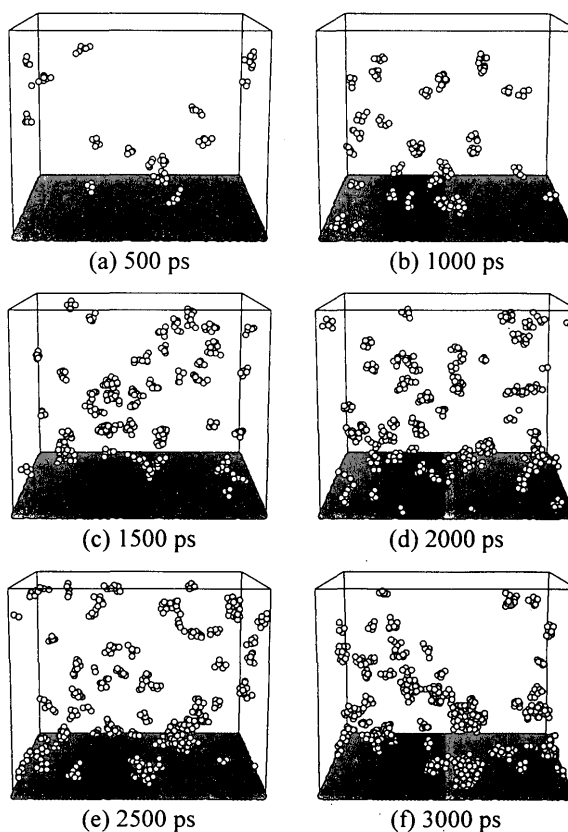


Figure 4 Snapshots of nucleation process for E1.

nucleation.

The cluster size distributions $c(n)$ for several instances (short-time average) are shown in Figure 5. Here, "On Surface" denotes that the distance between the surface and the nearest molecule of a cluster is smaller than $1.2\sigma_{INT}$. Compared to the natural equilibrium distribution in Figure 5 (a), constant amount of increase of distribution for the size range beyond $n = 10$ can be conceived. The cluster size distribution in the range $1 < n < 20$ seemed to keep the same structure after 1000 ps, it is also observed that, most of clusters beyond $n > 10$ are principally on surface for this wettability E2. The spikes in the larger cluster size range are due to small number of clusters further grew from this quasi-equilibrium distribution in the range $1 < n < 20$.

The variations of the numbers of clusters larger than some thresholds are shown in Figure 6 as in the same manner as the results of homogeneous nucleation by Yasuoka et al. [3]. Dashed lines were fitted to the linear part of each increasing curve by the least squares method. These lines are almost parallel for the thresholds of over 20 or 30 and it shows that the clusters exceeded that size keep to grow stably. The decay after linear increase was because of the coalescence of large clusters due to the limited calculation domain size. It was proposed that the nucleation rate is estimated from the gradients of these fitted lines [3]. Nucleation rate estimated from the average gradient of lines over 30, 40 and 50 becomes $J_{sim} = 3.45 \times 10^{21} \text{ cm}^{-2}\text{s}^{-1}$.

On the other hand, in the classical nucleation theory, nucleation rate J_{th} of the heterogeneous nucleation on the smooth solid surface is expressed as follows.

$$J_{th} = \rho^{\frac{2}{3}} \frac{\rho}{\rho_l} \frac{1 - \cos \theta}{2} \sqrt{\frac{2\gamma_{lv}}{\pi m f}} \exp\left(-\frac{\Delta G^*}{k_B T}\right) \quad (6)$$

$$f = \frac{1}{4}(2 - 3 \cos \theta + \cos^3 \theta)$$

$$\Delta G^* = \frac{16\pi^3 f}{3(\rho_l k_B T \ln S)^2}$$

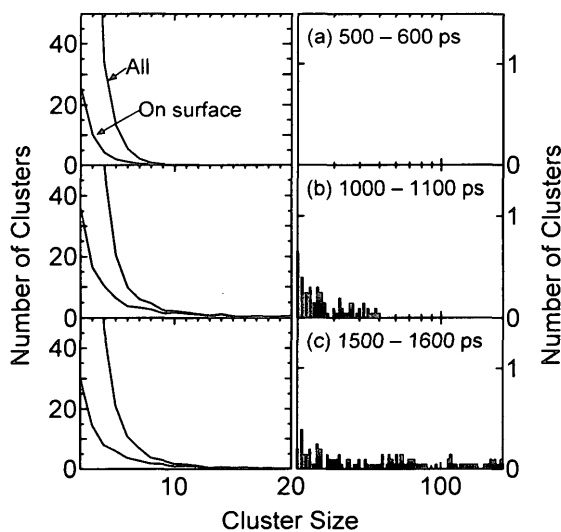


Figure 5 Clusters distribution for E2. Number of clusters is average number of scenes for 100 ps.

Using the average temperature T_{ave} and vapor density ρ in the period from 1000 ps to 1500 ps in which the number of clusters changed linearly in Figure 6, the nucleation rate was calculated to be $J_{th} = 4.47 \times 10^{21} \text{ cm}^{-2}\text{s}^{-1}$. Here, the values of the saturated vapor density ρ_e and liquid density ρ_l were calculated from the equation of state of Lennard-Jones fluid [8], and that of surface tension of liquid vapor interface γ_{lv} was employed from physical property of argon. Furthermore, the contact angle for each surface condition was estimated from our equilibrium simulation results [1]. The nucleation rate calculated from this simulation agreed with the classical nucleation theory very well in clear contrast to the 7 orders of difference for the homogeneous nucleation by Yasuoka et al. [3]. The critical cluster size in the classical nucleation theory is given in the following equation.

$$n^* = \frac{32\pi\gamma^3 f}{3\rho_l^2 (k_B T \ln S)^3} \quad (7)$$

It was calculated to be 16.5 in the case of E2. In this simulation, it was estimated to about 20 from the change of the gradients of the lines in Figure 6, and the agreement was reasonable.

Cluster size distribution in the range smaller than the critical nucleus n^* is given in following equation in the classical theory.

$$c(n) = \rho^{\frac{2}{3}} \exp\left(-\frac{\Delta G}{k_B T}\right) \quad (8)$$

The open circles in Figure 7 shows the free energy needed for cluster formation ΔG calculated using Eq. (8), from the average cluster distribution $c(n)$ such as in Fig. 5 in the period in which clusters were stably forming. The solid line shows ΔG given in the heterogeneous nucleation theory as follows.

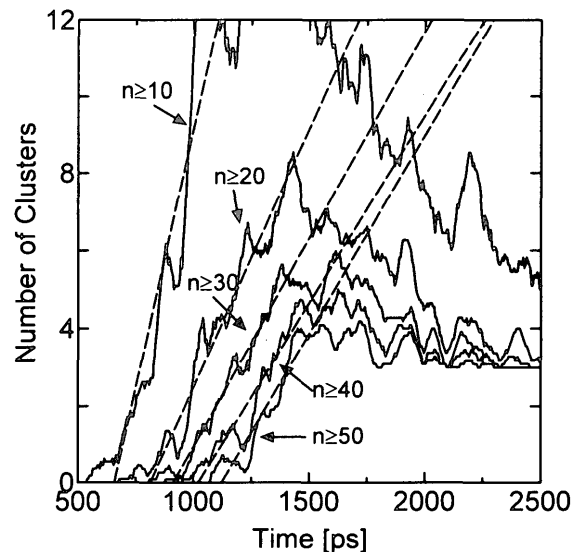


Figure 6 Variations of number of clusters larger than a threshold for E2 (short-time average).

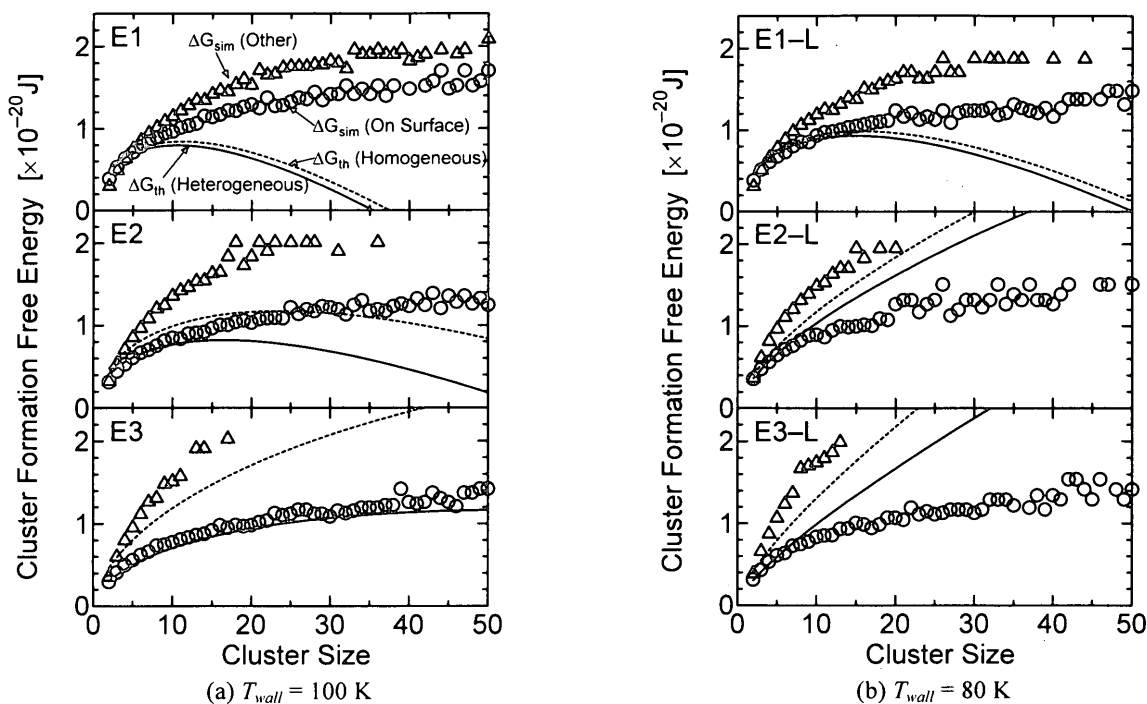


Figure 7 Cluster formation free energy for different temperature and various wettability (see Table 1 for the labels E1,E2,...). Circle and triangle symbols represent the estimation with Eq. (8) for “On Surface” and “Other”, respectively. Solid and broken lines represent corresponding classical nucleation theory.

$$\Delta G = \left(4\pi r^2 \gamma - \frac{4}{3}\pi r^3 \rho_l k_B T \ln S \right) f, \quad n = \frac{4}{3}\pi r^3 \rho_l f \quad (9)$$

Triangles and broken lines show ΔG calculated from cluster distribution far from solid surface and from the classical homogeneous nucleation theory, respectively. Considering that Eq. (8) is effective only in the size range smaller than the critical nucleus where ΔG is maximum in Eq. (9), it can be observed that ΔG from heterogeneous nucleation theory and from cluster distribution in contacted with solid surface almost agree for the simulations in which the set temperature of the solid surface T_{wall} was higher (100 K). Furthermore, ΔG from homogeneous nucleation theory and from cluster distribution far from the surface agreed well, though ΔG of simulation was slightly larger. The similar comparison of free energy by Yasuoka et al. [3] showed the remarkable difference in the simulation results from the classical theory.

On the other hand, for the simulations in which T_{wall} was lower (80 K), the difference between simulation and theory increased in E2-L and E3-L, though it almost agreed in E1-L whose surface was less wettable. Actually the theoretical value of the nucleation rate J_{th} for E2-L was extremely small value and the classical theory predicts no nucleation for the case of E3-L with the supersaturation ratio of 0.87. This discrepancy was because of the steep vertical temperature distribution in our simulations. The vertical temperature distributions in the period in which clusters were stably forming were calculated as shown in Figure 8. Considerably large temperature gradient has been given in E2-L and E3-L in which T_{wall} was lower and thermal

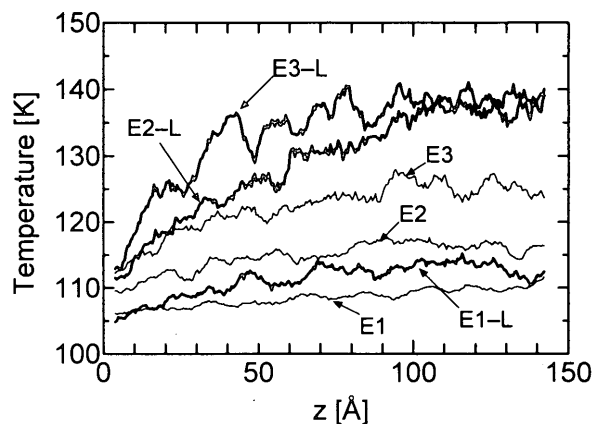


Figure 8 Temperature distribution during nucleation period.

boundary resistance [9] between liquid and solid surface was smaller than E1, E2 and E1-L. It can be understood that the difference from the classical nucleation theory tended to increase with the increase in the cooling rate because of the spatial temperature distribution.

5. CONCLUSION

We have successfully demonstrated the nucleation of 3-dimensional liquid droplet on the solid surface using the molecular dynamics method. Obtained nucleation rate,

the critical nucleus size and free energy needed for cluster formation almost agreed with classical heterogeneous theory in case that cooling rate was smaller or the solid surface was less wettable. Because of the spatial temperature distribution, the difference became larger with the increase in cooling rate and surface wettability.

6. ACKNOWLEDGEMENT

Part of this work was supported by Grand-in-Aid for Scientific Research (B) (No. 12450082) from the Ministry of Education, Science, Sports and Culture, Japan.

7. REFERENCES

1. Maruyama, S., Kurashige, T., Matsumoto, S., Yamaguchi, Y. and Kimura, T., Liquid Droplet in Contact with a Solid Surface, *Microscale Thermophysical Engineering*, Vol. 2, No. 1 (1998), pp. 49-62.
2. Maruyama, S. and Kimura, T., A Molecular Dynamics Simulation of a Bubble Nucleation on Solid Surface, *International Journal of Heat & Technology*, Vol. 18, No. 1 (2000), pp. 69-74.
3. Yasuoka, K. and Matsumoto, M., Molecular Dynamics of Homogeneous Nucleation in the Vapor Phase. I. Lennard-Jones Fluid, *Journal of Chemical Physics*, Vol. 109, No. 19 (1998), pp. 8451-8462.
4. Yasuoka, K. and Matsumoto, M., Molecular Dynamics of Homogeneous Nucleation in the Vapor Phase. II. Water, *Journal of Chemical Physics*, Vol. 109, No. 19 (1998), pp. 8463-8470.
5. Stoddard, S. D. and Ford, J., Numerical Experiments on the Stochastic Behavior of a Lennard-Jones Gas System, *Physical Review A*, Vol. 8 (1973), pp. 1504-1512.
6. Tully, J. C., Dynamics of Gas-Surface Interactions: 3D Generalized Langevin Model Applied to fcc and bcc Surfaces, *Journal of Chemical Physics*, Vol. 73, No. 4 (1980), pp. 1975-1985.
7. Blömer, J. and Beylich, A. E., Molecular Dynamics Simulation of Energy Accommodation of Internal and Translational Degrees of Freedom at Gas-Surface Interfaces, *Surface Science*, Vol. 423 (1999), pp. 127-133.
8. Nicolas, J. J., Gubbins, K. E., Streett, W. B. and Tildesley, D. J., Equation of State for the Lennard-Jones Fluid, *Molecular Physics*, Vol. 37, No. 5 (1979), pp. 1429-1454.
9. Maruyama, S. and Kimura, T., A Study on Thermal Resistance over a Solid-Liquid Interface by the Molecular Dynamics Method, *Thermal Science Engineering*, Vol. 7, No. 1 (1999), pp. 63-68.